Atmos. Chem. Phys., 5, 483–491, 2005
www.atmos-chem-phys.org/acp/5/483/
SRef-ID: 1680-7324/acp/2005-5-483
European Geosciences Union

Atmospheric Chemistry and Physics

Measurements of N_2O_5, NO_2, and O_3 east of the San Francisco Bay

E. C. Wood[1], **T. H. Bertram**[1], **P. J. Wooldridge**[1], **and R. C. Cohen**[1, 2, 3]

[1]Department of Chemistry, University of California, Berkeley, California
[2]Department of Earth and Planetary Sciences, University of California, Berkeley, California
[3]Energy and Environment Technologies Division, Lawrence Berkeley National Laboratory, Berkeley, California

Received: 13 September 2004 – Published in Atmos. Chem. Phys. Discuss.: 15 October 2004
Revised: 21 January 2005 – Accepted: 8 February 2005 – Published: 15 February 2005

Abstract. We report in situ measurements of N_2O_5, NO_2, and O_3 in Contra Costa County, California during January 2004. Mixing ratios of N_2O_5, an intermediate compound in the atmosphere's nocturnal cleansing process, ranged up to 200 pmol/mol at night. The highest N_2O_5 concentrations were correlated with low O_3 and high NO_2 concentrations. The calculated steady state lifetime for N_2O_5 ranged from 5 to 30 min. The total HNO_3 produced by N_2O_5 hydrolysis over a 14 h night was comparable to ambient NO_2 concentrations, and is estimated to be a factor of nine bigger than the HNO_3 produced during the day.

1 Introduction

The nitrate radical (NO_3) and dinitrogen pentoxide (N_2O_5) are uniquely important to the nocturnal chemistry of the troposphere. NO_3 is produced by the reaction of nitrogen dioxide (NO_2) with ozone (O_3):

$$NO_2 + O_3 \xrightarrow{k_1} NO_3 + O_2 \tag{1}$$

Reaction (1) is slow: at 278 K, k_1 is equal to 1.8×10^{-17} cm^3 molecule^{-1} s^{-1} (Sander et al., 2003), resulting in a 1/e lifetime for NO_2 at 30 nmol/mol (parts per billion by volume, ppbv) of O_3 of 24 h.

An equilibrium is established between NO_2, NO_3, and N_2O_5 on timescales of a few minutes:

$$NO_2 + NO_3 + M \longleftrightarrow N_2O_5 + M \tag{2}$$

In moderately cold and/or polluted conditions (i.e. high [NO_2]), this equilibrium is strongly shifted to the right. For example, at 10°C and 2 ppbv of NO_2, the [N_2O_5]:[NO_3] ratio at equilibrium is 11. This rapid removal of a second NO_2 molecule reduces the effective lifetime of NO_2 to 12 h. During the day, NO_3 is photolyzed (overhead photolysis rate $\approx$0.2 s^{-1}) and reacts rapidly with nitric oxide (NO), thus limiting NO_3 mixing ratios to well below 1 nmol/mol (parts per trillion by volume, pptv). In contrast, at night NO_3 mixing ratios of up to a few hundred pptv have been observed in urban plumes (Wayne et al., 1991) and mixing ratios up to 40 pptv are common in more remote regions (Brown et al., 2003a; Carslaw et al., 1997; Geyer et al., 2001; Simpson, 2003; Wayne et al., 1991). N_2O_5 mixing ratios of up to 3 ppbv have been observed near Boulder, Colorado (Brown et al., 2003a). In northern latitudes (Simpson, 2003) and in the marine boundary layer (Brown et al., 2004) N_2O_5 mixing ratios of less than 0.1 ppbv are more common.

The chemistry of NO_3 and N_2O_5 affects the concentrations of volatile organic compounds (VOCs) and NO_x ($NO_x \equiv NO+NO_2$). NO_3 reacts rapidly with alkenes and calculations suggest that NO_3 is the predominant oxidant for some biogenic VOCs (Warneke et al., 2004; Wayne et al., 1991). N_2O_5 hydrolyzes on surfaces to form nitric acid (HNO_3):

$$N_2O_5 + H_2O_{(l)} \xrightarrow{\text{heterogeneous}} 2HNO_3 \tag{3}$$

The set of Reactions (1–3) is one of the major paths for the removal of NO_x from the atmosphere. The sticking coefficient (γ) for Reaction (3) varies from 0.02 for uptake onto $NaNO_3$ aerosol (Mentel et al., 1999) to over 0.1 for uptake onto H_2SO_4 aerosol (Hanson and Ravishankara, 1991; Robinson et al., 1997). Measurements in a variety of locations have indicated that the NO_2 removed at night by Reactions (1–3) can be comparable in magnitude to the loss of NO_2 during the day by reaction with OH to form nitric acid (Heintz et al., 1996; Martinez et al., 2000).

Prior to 2000, atmospheric N_2O_5 had only been measured by long-path absorption spectroscopy in the stratosphere (Kunde et al., 1988; Rinsland et al., 1989; Sen et al., 1998; Toon et al., 1986; Zhou et al., 1997), and NO_3

Correspondence to: R. C. Cohen
(cohen@cchem.berkeley.edu)

Fig. 1. Map of the greater San Francisco Bay Area. The Leuschner observatory is indicated by the arrow (adapted from http://www.sfgate.com/traveler).

had only been measured by Differential Optical Absorbance Spectrometry (DOAS) (Heintz et al., 1996; Platt and Heintz, 1994) and Matrix Isolation-Electron Spin Resonance Spectrometry (MI-ESR) (Geyer et al., 1999). More recently, in situ instruments based on Cavity Ring-Down Spectroscopy (CRDS) have been constructed (Brown et al., 2002; Simpson, 2003). These CRDS instruments have superior sensitivity to NO_3 and have produced the first measurements of tropospheric N_2O_5. We recently described our approach to measurement of NO_3 and N_2O_5 by laser-induced fluorescence (LIF) (Wood et al., 2003). In this manuscript we describe the first field test of this instrument.

2 Experimental

Concentrations of N_2O_5, NO_2, O_3, and meteorological data were measured at the Leuschner Astronomical Observatory on the University of California Russell Reservation in Contra Costa County, California (37:55:06° N, 122:9:24° W, altitude 290 m) during January 2004 (Fig. 1). The reservation is a 115 hectare site consisting of a mix of forest, woodland, chaparral, and grassland vegetation. To the north is the 2300 hectare Briones Regional Park. The city center of Lafayette, a suburban town 30 km northeast of San Francisco, is 4 km southeast of the site. Highway 24, on which there is moderate traffic at night, passes 3 km to the south of the site. Extending from the southwest to the northeast along highway 80 and highway 4 are a number of oil refineries and natural gas-fired power plants, at closest 10 km to the site.

2.1 N_2O_5 measurements

N_2O_5 was measured by LIF detection of NO_3 after thermal dissociation to NO_2 and NO_3:

$$N_2O_5 + M \xrightarrow{\Delta} NO_2 + NO_3 + M \tag{4}$$

using an instrument based on the prototype described in Wood et al. (2003). Although this method yields a measurement of the sum of ambient $[NO_3]$ and $[N_2O_5]$, due to the high $[N_2O_5]$:$[NO_3]$ ratios expected at the ambient temperatures and NO_2 concentrations observed, we interpret all measurements as N_2O_5. For example, at 3°C and 5 ppbv of NO_2 (typical conditions for the data presented in Sect. 3), the $[N_2O_5]$:$[NO_3]$ ratio, calculated from the equilibrium constant of Reaction (2), is 80. NO_3 ranged from 0.5%–10% of the measured sum in this dataset, and was usually less than 5% of the sum.

The support equipment (e.g. gas tanks and computer) was located in the observatory and the laser, detection cell, electronics, and vacuum pumps were situated outside, 3 m from the observatory. Air was sampled at a height of 1.2 m. A 6 standard liters/min (SLPM) flow of ambient air passed through a 22 cm section of 3/8″ OD PFA Teflon tubing resistively heated to an external temperature of 190°C. Sampled air had a 70 ms transit time in the heated region before passing through an 0.8 mm orifice into the detection region, which was held at 2 Torr (2.7 mbar). Varing the inlet temperature from ambient to 200°C indicated that N_2O_5 was fully dissociated at 170° under these conditions. The cell pressure was measured with a capacitance manometer (MKS).

Figure 2 depicts the optical cell and inlet of the instrument. NO_3 was excited by 662 nm light from a high-power (300 mW), multi-mode (bandwidth=0.3 nm) InAlGaP diode laser in the $B^2\mathrm{E}'$ (0000)$\leftarrow X^2\mathrm{A}_2'$ (0000) band. An aspheric lens focused the diode output from the 1 μm×150 μm emitting strip to an 0.3 cm (horizontal) by 1 cm (vertical) rectangular spot at the center of the cell. The laser light entered the cell through a glass window mounted at 45° located 20 cm from the center of the cell and exited through a similar glass window 13 cm from the center. Vertical slit geometric baffles were used to reduce laser scatter and to exclude ambient light from the cell. The laser power exiting the cell was monitored by a photodiode. The electric field vector of the laser light was aligned parallel to the detection axis in order to minimize the collection of Rayleigh, Raman, and other polarized scattered laser light. NO_3 fluorescence was collected by a 55 mm focal length lens and passed through a 750 nm short-pass filter, an all dielectric 700 nm long-pass interference filter, and a second 700 nm long-pass interference filter which contained a layer of absorbing glass. The final filtered fluorescence was focused onto the photocathode of a thermoelectrically-cooled red-sensitive GaAs Hamamatsu H7421-50 photomultiplier tube (PMT).

The high laser power, single-pass design of this instrument had comparable sensitivity to the low laser power, multi-pass design of the prototype described in Wood et al. (2003). The background of this single-pass design (∼100 counts/s) was 14 times smaller than that of the prototype. The signal rate was half that of the prototype; the reduction in laser fluence due to foregoing a multi-pass alignment was almost compensated for by the increase in laser power. The poor beam quality of this laser precluded use of a multipass arrangement.

The instrument's background was measured by injection of NO into the inlet, which converts NO_3 to NO_2:

$$NO + NO_3 \longrightarrow 2NO_2 \qquad (5)$$

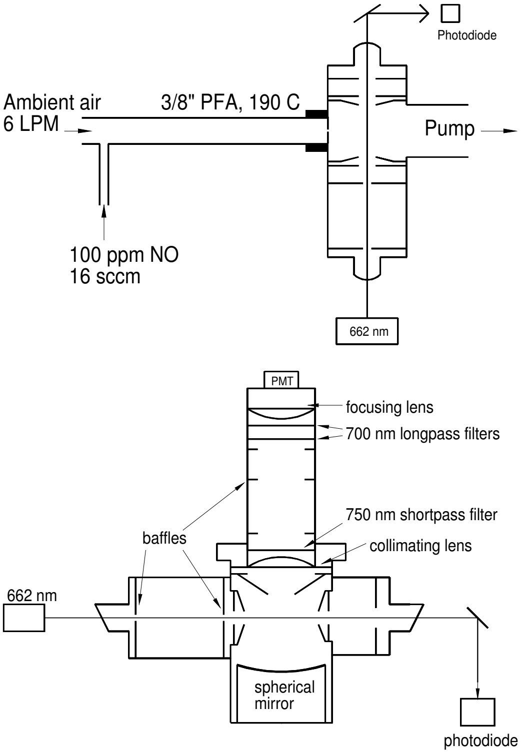

Fig. 2. (a) Schematic diagram of the N_2O_5 LIF instrument's gas flow and excitation axes. Ambient air passes through 22 cm of 3/8″ OD PFA teflon tubing which is externally heated to 190°C. After a 70 ms residence time, the air expands through a 0.8 mm orifice into the optical cell where the NO_3 from the thermal decomposition of N_2O_5 is excited by 300 mW of 662 nm light from a diode laser. **(b)** Schematic diagram of the excitation and detection axes. NO_3 fluorescence between 700 and 750 nm is imaged onto the photocathode of a cooled red-sensitive PMT. The spherical mirror acts as a retroreflector and almost doubles the optical collection efficiency of the optical cell. A series of geometric baffles and spectral filters reduces the background to 100 counts/s.

The NO (Scott Specialty Gas) flowed through a $FeSO_4$ trap in order to convert impurity NO_2 into NO. We used a 16 standard cubic cm^3/min (sccm) flow of 100 ppmv NO delivered through a mass flow controller (MKS) and a solenoid valve to a PFA tee at the mouth of the inlet. The concentration of NO used (270 ppbv after dilution into the main flow of 6000 sccm) was sufficient to react >99% of the NO_3 while reacting with less than 1% of ambient O_3. The experimental procedure consisted of 10 s of background observation (with NO flowing into the inlet) followed by 15 s of N_2O_5 observation. Data from the first five of these 15 s were discarded to ensure no contamination of the data by leaking of NO into the ambient air flow. Standard additions of N_2O_5 (6 sccm, 1 ppmv diluted into a total flow of 6000 sccm) confirmed that leaking of NO was negligible two seconds after the solenoid valve closed. There is a small amount of NO_2 fluorescence following 662 nm excitation. Since NO_2 is present during both the background and sampling periods, this is accounted for in the background measurement.

The instrument background was typically between 105 and 115 PMT counts/s, of which 5 were from the PMT dark current, 75 were from laser scatter, 20 were from O_2 Stokes Raman scattering, and at most 1 was from NO_2 fluorescence (at 20 ppbv of NO_2). The remainder were presumably from Mie scattering and/or fluorescence of ambient aerosol. This aerosol component was pressure-dependent and only observed while sampling ambient air and not "zero" air (medical grade compressed air). The magnitude and variance of this scattering was as much as seven times higher with the inlet set at ambient temperature than at 190°C and was highest during nights of high relative humidity. The high variability of this component of the background necessitated the 10 s off/15 s on measurement cycle described above. Measurements were not possible on occasional nights of visibly high optical extinction (e.g. fog) due to excessive noise in the background. Teflon membrane filters eliminated this aerosol scattering and transmitted over 98% of N_2O_5. However, with the filter in place the pressure of the cell decreased over time, indicating that deposition of significant amounts of particulate matter was clogging the filter. This pressure decrease was fast enough that use of the filter would have required hourly filter changes and raised questions about N_2O_5 transmission over time that were avoided by the fast background-sampling cycle.

By slowly increasing the pressure in the cell while sampling ambient air, this Mie scattering was quantified and served as a relative measurement of the ambient aerosol load. The slope of the plot of PMT counts s^{-1} versus pressure varied from 12 counts s^{-1} $Torr^{-1}$ to 60 counts s^{-1} $Torr^{-1}$, of which 10 counts s^{-1} $Torr^{-1}$ were from O_2 Raman scattering (measured with zero air overflowing the inlet). The slope obtained while overflowing the inlet with zero air was used to track changes in the calibration constant (see below).

The instrument was calibrated in the laboratory at the conclusion of the field campaign as described in Wood et al. (2003). A mixture of N_2O_5 and NO_2 was delivered to the instrument's heated inlet and the resultant NO_3 fluorescence was observed. The NO_2 concentration was quantified by LIF using a 15 mW, tunable diode laser at 408 nm. The spectral modulation used with the 638 nm laser described in Wood et al. (2003) to distinguish the NO_2 fluorescence from the NO_3 fluorescence was unnecessary with this violet laser as NO_3 does not fluoresce after excitation at 408 nm (Johnston et al., 1996). Finally, NO was added to the inlet and the increase in NO_2 signal from the reaction of NO with NO_3 was used to quantify the NO_3 concentration. Heterogeneous losses of NO_3 within the inlet were accounted for by this method of calibration since the NO_3 was rapidly converted to NO_2, which passes into the optical cell without losses. Heterogeneous losses of N_2O_5 were estimated to be negligible based on the the wall loss rate constant of 8×10^{-3} s^{-1} measured by Simpson for N_2O_5 on 1/2″ OD dry PFA tubing at 1 atm (Simpson, 2003). Differences in heterogeneous losses between laboratory and field conditions associated with humidity were expected to be small as the inlet air was kept hot and therefore at low relative humidity. Electronic quenching of excited NO_3 by water vapor was shown to be no more significant than that by nitrogen or oxygen: during a standard addition of N_2O_5 to the inlet, no discernable difference in fluorescence (<1%) was observed when the N_2O_5 flow (10 sccm) was diluted with dry zero air or with ambient air of 95% relative humidity at 11°C (χ_{water}=1.2%).

In addition to continuous measurement of the laser power throughout the field experiments, the instrument's Raman scattering sensitivity was measured nightly by overflowing the inlet with zero air and gradually increasing the cell pressure. The slope of the plot of PMT counts s^{-1} versus cell pressure quantified the O_2 Raman scattering at 739 nm (the Q-branch of the N_2 Stokes Raman scattering occurs on the long wavelength side of the 750 nm short-pass filter). Variations in the O_2 Raman scattering intensity were used to track any changes in the optical collection efficiency of the instrument. The in-field calibration constant for each night was deduced by examination of the laser power and this Raman slope. During the course of the experiment (∼1 month), the laser power decreased from 333 to 108 mW and the calibration constant decreased from 86 to 28 counts s^{-1} $ppbv^{-1}$. With a background of 110 counts/s and a calibration constant of 43 counts s^{-1} $ppbv^{-1}$ (typical values for the measurements presented in the results section below), the detection limit for N_2O_5 was 28 pptv in a 10 min integration (signal-to-noise=2). The total uncertainty was estimated to be under 15%.

2.2 Other measurements

NO_2 was measured by laser-induced fluorescence using the instrument described by Cleary et al (Cleary et al., 2002). Briefly, ambient air was transported through four meters of 1/4″ OD PFA Teflon tubing to the instrument which was housed inside the observatory. Air was pumped through a 350 μm orifice into a chamber held at 300 mTorr, producing a supersonic expansion. Light from a 6 mW tunable diode laser (TUI optics) at 640 nm excited the rotationally cooled NO_2 in the ($A^2B_2 \leftarrow X^2A_1$) transition. The laser light intersected the supersonic expansion ∼1 cm downstream of the nozzle in a 72-pass Herriott cell alignment. Fluorescence to the red of 750 nm was detected by a GaAs PMT. The accuracy and detection limit of this instrument were 5% and 140 pptv (60-s average, signal-to-noise=2), respectively. The decrease in laser power since the publication of Cleary et al (6 mW vs 16 mW) was offset by the discovery of an NO_2 line with twice the intensity of that previously used.

Ozone was measured by absorption of 254 nm light using a Dasibi 1008-RS analyzer, which had an accuracy of 1% and a detection limit of 1 ppbv with 1 min averaging. Relative humidity, wind direction and speed were measured with

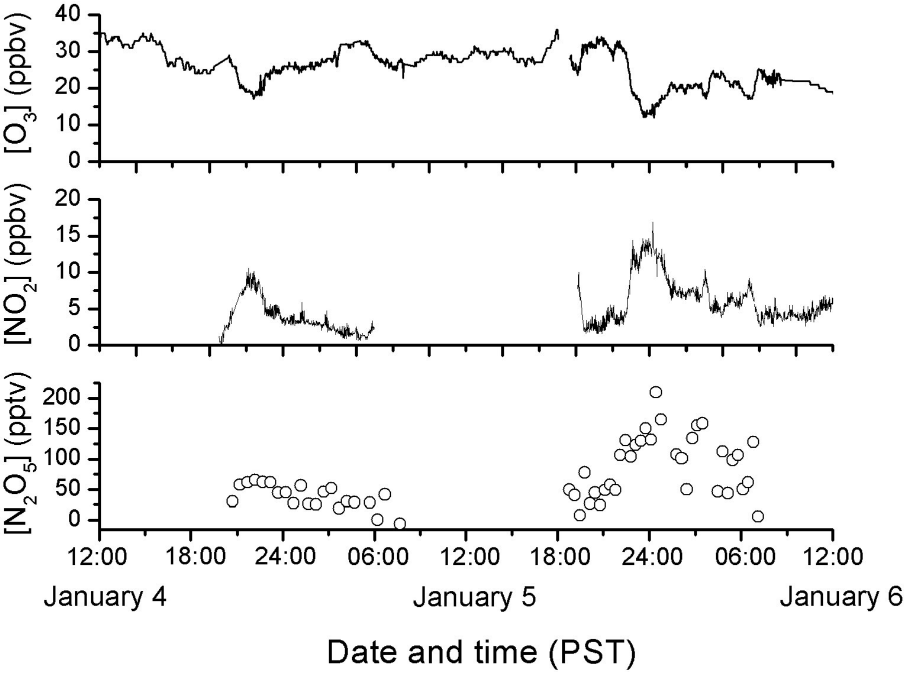

Fig. 3. Time series of [O_3] (1 min average), [NO_2] (30 s average), and [N_2O_5] (30 min average) from 4 January 2004–6 January 2004.

a Texas Weather instruments WR-25 weather station on the roof of the observatory. Air temperature was measured 15 m outside the observatory.

3 Results

Measurements were taken on six nights during January 2004. Temperatures ranged from 2°–12°C with the relative humidity usually between 70% and 100% (fog). Winds were usually calm (less than 2 m/s) and had no regular direction. N_2O_5 mixing ratios were above the detection limit (6 pptv in a 1 h integration at full laser power) on only a few of these nights, and were at most 200 pptv. The nights when [N_2O_5] was below the detection limit were characterized by either high relative humidity (>90%, occasionally foggy), ozone mixing ratios below 12 ppbv, or uncharacteristically low NO_2 mixing ratios (<1 ppbv).

A time series of NO_2, O_3, and N_2O_5 for the nights of 4 and 5 January is shown in Fig. 3. On the night of the 4th the temperature was 3±1°C, the relative humidity was 70–75%, the wind speed was 0–2 m/s and the wind direction was variable. On the night of the 5th the temperature was 6.5±0.5°C with 1–2 m/s winds from the north/northeast giving way to westerly winds shortly before midnight. The relative humidity increased shortly after this change in wind direction from 55% to 73%. Ozone mixing ratios varied from 15–35 ppbv and N_2O_5 ranged up to 200 pptv during these two nights. The observed scatter in the N_2O_5 time series is a combination of atmospheric variability and instrumental noise (the 1σ precision for 30 min averages is 9 pptv). The highest N_2O_5 concentrations were observed during the transit of plumes observed from 20:30–24:00 Pacific Standard Time (PST) on 4 January and 20:30–04:20 PST on 5 and 6 January that exhibited high NO_2 and low O_3 concentrations. N_2O_5 concentrations decayed to zero shortly after local sunrise at 07:20 PST on the morning of 6 January. Instrumental failures prevented measurement of N_2O_5 or NO_2 during sunrise on 5 January. Measurements did not resume until the evening of 5 January.

The quantity F(NO_{SUM}), using the terminology of Brown et al. (2003a), represents the fraction of reactive nitrogen oxides in the form of N_2O_5 or NO_3 and is defined as ([NO_3]+2[N_2O_5])/([NO]+[NO_2]+[NO_3]+2[N_2O_5]). At these low NO_3 concentrations and in the assumed absence of NO, F(NO_{SUM}) is equal to 2[N_2O_5]/(2[N_2O_5]+[NO_2]) and was usually in the range 0.01–0.04.

Given ample time, a pseudo steady state is formed between the production of NO_3 and N_2O_5 and their losses (e.g. hydrolysis of N_2O_5). The N_2O_5 steady state lifetime is defined as

$$\tau_{SS}(N_2O_5)=\frac{[N_2O_5]}{k_1[NO_2][O_3]} \tag{6}$$

In the absence of direct NO_3 losses, this lifetime is equal to the reciprocal of the first order N_2O_5 loss rate constant as described by Brown et al. (2003b). Direct losses of NO_3 are not expected to be significant since the scavengers of NO_3 were expected to be scarce: NO is converted to NO_2 at night by reaction with O_3, and biogenic hydrocarbons are not expected in significant concentrations at this site in winter.

The pseudo steady state lifetimes of N_2O_5 calculated from the measurements on the nights of 4 and 5 January range from 10 to 30 min. Although it is possible for the steady state to be disrupted by NO emissions, this was unlikely. The nearest significant NO_x source was highway 24, which is 3 km south of the site. At a speed of 2 m/s it would take 25 min for such air to reach the site, a time comparable to that required for the formation of the steady state. Also, since traffic on highway 24 was low at night and winds were rarely observed from the south, the more likely NO_x sources were from the more distant power plants to the north of the site (e.g. in Martinez, 10 km away). Soil emissions of NO were unlikely due to the cold temperatures (Meixner and Yang, 2004). If there were a small NO source close to the measurement site, however, the N_2O_5 lifetimes calculated by Reaction (6) would be underestimates of the true N_2O_5 lifetime due to hydrolysis. As an estimate of the potential error from this term, we calculate the effect of a high concentration of NO, 10 pptv, on the calculated lifetime of N_2O_5. For an N_2O_5 loss rate constant of $(20\,\text{min})^{-1}$ with initial values of $[NO_2]$ of 8 ppbv and $[O_3]$ of 25 ppbv, we find that the lifetime calculated using Reaction (6) would be in error by $\approx$15%. Anthropogenic alkenes would have to exist in unrealistically high concentrations to have a comparable effect since their rate constants for reaction with NO_3 are orders of magnitude slower than the rate constant for the reaction of NO with NO_3. For example, 30 ppbv of propene would be required to have the equivalent effect of 10 pptv of NO.

Strong vertical concentration gradients caused by the emission of NO, as observed by DOAS (Stutz et al., 2004), are not likely here in the absence of a nearby NO source. Any vertical gradient produced in an air parcel at the distant NO sources would most likely have disappeared during advection to the measurement site. However, it is possible that direct deposition to the surface could be a sink of N_2O_5 that contributes to a vertical gradient, although we calculate that the N_2O_5 lifetime with respect to deposition is several hours, which is an order of magnitude longer than the lifetime we infer from the observations.

On nights when the N_2O_5 mixing ratios were below the detection limit, an upper limit can be calculated for $\tau_{SS}(N_2O_5)$. For example, on 10 and 11 January, $[NO_2]$ was on average 1.5 ppbv, $[O_3]$ was 31 ppbv, and the relative humidity was 89%. Assuming a maximum N_2O_5 mixing ratio of 6 pptv, the calculated steady state lifetime was at most 5 min. The aerosol scattering this night, as measured by the pressure dependence of the instrument's background, was twice that measured the night of the 4th.

4 Discussion

The pseudo steady state lifetime of N_2O_5 is an indication of the role of NO_3 and N_2O_5 in an air mass. Long lifetimes indicate that N_2O_5 is relatively unreactive and is mainly a nocturnal reservoir of NO_x, re-forming NO_x in the morning after thermal decomposition of N_2O_5 and subsequent photolysis of NO_3. Shorter lifetimes indicate higher reactivity of N_2O_5 and its role as a sink for NO_x. Correlations of the pseudo steady state lifetime with relative humidity and aerosol load have been used at numerous locations to infer the mechanism of N_2O_5 loss. At a site near Boulder, Colorado in November of 2001, Brown and co-workers observed N_2O_5 in an urban plume with $[NO_2]$ and $[O_3]$ comparable to those we report here (Brown et al., 2003a, b). Their observed N_2O_5 mixing ratios were much larger ($F(NO_{SUM})$ up to 0.25) than observed at Leuschner, and calculations using their data give an N_2O_5 steady state lifetime of approximately 2 h. The measurement site in Colorado was typically characterized by relative humidity values below 60% at night.

In the marine boundary layer off the coast of New England during the summer of 2002, N_2O_5 mixing ratios measured by Brown et al were much smaller (<200 pptv) and $F(NO_{SUM})$ was on average 0.05 (Brown et al., 2004). The N_2O_5 pseudo steady state lifetime was on order 30 min to 1 h, in an environment in which there were significant losses of NO_3 due to reaction with dimethyl sulfide and biogenic hydrocarbons (Warneke et al., 2004).

Using measurements of NO_3, NO_2, O_3, and the aerosol size distribution in Helgoland, Germany during October 1996, Martinez et al inferred the N_2O_5 pseudo steady state lifetime and demonstrated a negative correlation with the aerosol load (Martinez et al., 2000). The N_2O_5 steady state lifetimes ranged from 8 to 15 min at aerosol surface area values of 500–700 $\mu m^2\,cm^{-3}$ and 15 min to 120 min at aerosol surface areas less than 200 $\mu m^2\,cm^{-3}$. The negative correlation of $\tau_{SS}(N_2O_5)$ with the average aerosol radius was more pronounced than that with aerosol surface area, which they attributed to the fact that the more N_2O_5-reactive deliquescent particles can grow to large diameters due to uptake of water.

N_2O_5 steady state lifetimes were calculated from observations of NO_3, NO_2, and O_3 at a rural site in the Baltic Sea over a period of 14 months (Heintz et al., 1996). The N_2O_5 steady state lifetimes varied from 17 min to over 5 h, though they were usually under an hour. Additionally, a negative correlation between the NO_3 lifetime and $[NO_2]$, which is usually presented as evidence of the predominance of N_2O_5 loss over NO_3 loss mechanisms (Geyer et al., 2001; Martinez et al., 2000), was only found to exist for relative humidities above 58%.

Heterogeneous loss of N_2O_5 on the surface of aerosols is expected to be an important sink in the conditions observed at the Leuschner Observatory. The relative humidity was usually greater than 75%, which is near the deliquescence relative humidity of many common aerosol systems, suggesting that most aerosol particles were in the liquid phase. Uptake of N_2O_5 is in general much faster onto aqueous aerosol than onto solid aerosol (e.g. $\gamma(N_2O_5)$ onto $(NH_4)_2SO_4$ aerosol is

2×10^{-3} at 20% relative humidity and 1.5×10^{-2} at 70% relative humidity; Hallquist et al., 2003).

For aerosol radii less than 1 μm the N_2O_5 loss rate constant (k_{het}) due to heterogeneous uptake onto aerosol can be expressed as

$$k_{het} = \tau^{-1}(N_2O_5) = \gamma A\bar{c}/4 \tag{7}$$

where γ is the uptake coefficient of N_2O_5 and is a function of the aerosol composition, A is the surface area density, and $\bar{c}$ is the mean molecular speed of N_2O_5. At 279 K, a lifetime of 20 min with a γ of 0.07 corresponds to an aerosol surface area density of 200 μm^2 cm^{-3}, a reasonable estimate and one consistent with the relationships between the N_2O_5 lifetime and aerosol load observed by Martinez et al. The low N_2O_5 concentrations and short lifetimes (<5 min) observed at the Leuschner Observatory on nights of high relative humidity (>90%) are consistent with a reactive high surface area due to the growth of deliquescent particles by uptake of water.

As a result of the short N_2O_5 lifetime, nearly all of the NO_2 converted to NO_3 and N_2O_5 by Reactions (1) and (2) will be irreversibly converted to HNO_3 during the night. The total amount of nitric acid produced over the course of the 14 h night can estimated by assuming that each molecule of NO_3 formed by Reaction (1) will react to form N_2O_5, which in turn hydrolyzes to form two molecules of HNO_3. The total HNO_3 is then equal to twice the integrated rate of Reaction (1):

$$[HNO_3]_{total} = 2\int \frac{[N_2O_5]}{\tau_{SS}(N_2O_5)}dt = 2\int k_{NO_2+O_3}[NO_2][O_3]dt \tag{8}$$

Calculated $[HNO_3]_{total}$ values ranged from 1.4 ppbv to 5.9 ppbv during this experiment. For example, on the night of the 4th, $[HNO_3]_{total}$ was calculated to be 4.1 ppbv. Note that this is comparable to the average NO_2 mixing ratio that night, indicating that this loss of NO_x was balanced by fresh emissions on the regional scale.

The ratio of heterogeneous HNO_3 production to that produced by the reaction of OH with NO_2 during the day can be estimated:

$$\frac{\int HNO_3(\text{night})}{\int HNO_3(\text{day})} = \frac{\int 2k_{NO_2+O_3}[NO_2][O_3]dt}{\int k_{OH+NO_2}[OH][NO_2]dt} \tag{9}$$

At the measurement site in January there was little difference between daytime and nighttime NO_2 concentrations, and thus the NO_2 term cancels out. Using the average nocturnal ozone mixing ratio of 25 ppbv, an estimated average daytime OH concentration of 3.4×10^5 molecules cm^{-3} (Spivakovsky et al., 2000), values of 1.7×10^{-17} cm^3 $molecule^{-1}$ s^{-1} for k_{NO2+O3} and 10^{-11} cm^3 $molecule^{-1}$ s^{-1} as the effective bimolecular rate constant for k_{OH+NO2} at 279 K, and integrating over 14 h for the night and 10 h for the day yields a ratio of 9.

The nocturnal removal of NO_x via N_2O_5 hydrolysis is likely occurring over a volume comparable to that under which the daytime removal of NO_2 occurs during the winter. The lifetime of NO_2 due to reaction with 3.4×10^5 molecules cm^{-3} OH is 3 days, and so most daytime NO_2 will persist into the residual layer at night, where it can undergo the same chemistry as observed in the nocturnal boundary layer. Thus differences in boundary layer height between day and night are unlikely to affect the significance of the ratio calculated in Reaction (9). This is in contrast to expectations for summer when the daytime concentration of OH is likely an order of magnitude higher, reducing the lifetime of NO_2 to reaction with OH to less than 10 h. Thus much less NO_2 will persist into the residual layer, and N_2O_5 hydrolysis will be limited to the nocturnal boundary layer, lowering its overall importance.

5 Conclusions

Measurements of N_2O_5, NO_2, and O_3 at the University of California Russell Reservation in Contra Costa County, California indicate that N_2O_5 is very reactive at this location, with the steady state lifetimes for N_2O_5 no longer than 30 min. Heterogeneous hydrolysis to form HNO_3 is the most likely loss process, and thus formation of NO_3 and N_2O_5 represents a sink of NO_x since HNO_3 is rapidly removed from the atmosphere by wet or dry depostion. Future measurements of N_2O_5 alongside an extended suite of complementary measurements including NO, VOCs, aerosol composition and size, and HNO_3 will allow for a more quantitative understanding of the individual losses of NO_3 and N_2O_5 and the subsequent fate of HNO_3. Other issues to be explored include the oxidation of VOCs by NO_3 during the warmer seasons to form alkyl nitrates (measurable by TD-LIF; Day et al., 2002) and the role of NO_3 and N_2O_5 as a sink of odd oxygen, O_x ($O_x \equiv O_3+NO_2+2NO_3+3N_2O_5$).

Although this first field test of our N_2O_5 LIF instrument was succesful, the time-varying component of the instrument background caused by aerosol scattering precluded its use at conditions of high aerosol load. Future improvements to the instrument, foremost the implementation of pulsed excitation and delayed time-gated detection, will eliminate this component and reduce other components of the background, enabling measurement of N_2O_5 and possibly NO_3 in a wider range of environments.

Acknowledgements. We thank J. Graham of the University of California-Berkeley Astronomy department for help in choosing a measurement site, C. Bresloff for coordinating our use of the Leuschner Observatory, and A. Goldstein of the Environmental Science, Policy, and Management department for the loan of the Dasibi ozone monitor. This work was funded by NSF grant No. 0138669.

Edited by: A. Hofzumahaus

References

Brown, S. S., Stark, H., Ciciora, S. J., McLaughlin, R. J., and Ravishankara, A. R.: Simultaneous in situ detection of atmospheric NO_3 and N_2O_5 via cavity ring-down spectroscopy, Rev. Sci. Ins., 73 (9), 3291–3301, 2002.

Brown, S. S., Stark, H., Ryerson, T. B., Williams, E. J., Nicks, D. K., Trainer, M., Fehsenfeld, F. C., and Ravishankara, A. R.: Nitrogen oxides in the nocturnal boundary layer: Simultaneous in situ measurements of NO_3, N_2O_5, NO_2, NO, and O_3, J. Geophys. Res.-A, 108 (D9), 4299, doi:10.1029/2002JD002917, 2003a.

Brown, S. S., Stark, H., and Ravishankara, A. R.: Applicability of the steady state approximation to the interpretation of atmospheric observations of NO_3 and N_2O_5, J. Geophys. Res.-A, 108 (D17), 4539, doi:10.1029/2003JD003407, 2003b.

Brown, S. S., Dibb, J. E., Stark, H., Aldener, M., Vozella, M., Whitlow, S., Williams, E. J., Lerner, B. M., Jakoubek, R., Middlebrook, A. M., DeGouw, J. A., Warneke, C., Goldan, P. D., Kuster, W. C., Angevine, W. M., Sueper, D. T., Quinn, P. K., Bates, T. S., Meagher, J. F., Fehsenfeld, F. C., and Ravishankara, A. R.: Nighttime removal of NO_x in the summer marine boundary layer, Geophys. Res. Lett., 31 (8), L07108, doi:10.1029/2004GL019412, 2004.

Carslaw, N., Plane, J. M. C., Coe, H., and Cuevas, E.: Observations of the nitrate radical in the free troposphere at Izana de Tenerife, J. Geophys. Res., 102 (D9), 10 613–10 622, 1997.

Cleary, P. A., Wooldridge, P. J., and Cohen, R. C.: Laser-induced fluorescence detection of atmospheric NO_2 with a commercial diode laser and a supersonic expansion, Appl. Opt., 41 (33), 6950–6956, 2002.

Day, D. A., Wooldridge, P. J., Dillon, M. B., Thornton, J. A., and Cohen, R. C.: A thermal dissociation laser-induced fluorescence instrument for in situ detection of NO_2, peroxy nitrates, alkyl nitrates, and HNO_3, J. Geophys. Res.-A, 107 (D5–D6), art. no. 4046, doi:10.1029/2001JD000779, 2002.

Geyer, A., Alicke, B., Mihelcic, D., Stutz, J., and Platt, U.: Comparison of tropospheric NO_3 radical measurements by differential optical absorption spectroscopy and matrix isolation electron spin resonance, J. Geophys. Res.-A, 104 (D21), 26 097–26 105, 1999.

Geyer, A., Ackermann, R., Dubois, R., Lohrmann, B., Muller, T., and Platt, U.: Long-term observation of nitrate radicals in the continental boundary layer near Berlin, Atmos. Envir., 35 (21), 3619–3631, 2001.

Hallquist, M., Stewart, D. J., Stephenson, S. K., and Cox, R. A.: Hydrolysis of N_2O_5 on sub-micron sulfate aerosols, Phys. Chem. Chem. Phys., 5 (16), 3453–3463, 2003.

Hanson, D. R. and Ravishankara, A. R.: The Reaction Probabilities of $ClONO_2$ and N_2O_5 on 40-Percent to 75-Percent Sulfuric-Acid-Solutions, J. Geophys. Res.-A, 96 (D9), 17 307–17 314, 1991.

Heintz, F., Platt, U., Flentje, H., and Dubois, R.: Long-term observation of nitrate radicals at the Tor Station, Kap Arkona (Ruegen), J. Geophys. Res., 101 (D17), 22 891–22 910, 1996.

Johnston, H. S., Davis, H. F., and Lee, Y. T.: NO_3 Photolysis Product Channels – Quantum Yields From Observed Energy Thresholds, J. Phys. Chem., 100 (12), 4713–4723, 1996.

Kunde, V. G., Brasunas, J. C., Maquire, W. C., Herman, J. R., Massie, S. T., Abbas, M. M., Herath, L. W., and Shaffer, W. A.: Measurement of Nighttime Stratospheric N_2O_5 from Infrared Emission Spectra, Geophys. Res. Lett., 15, 1177–1180, 1988.

Martinez, M., Perner, D., Hackenthal, E. M., Kulzer, S., and Schutz, L.: NO_3 at Helgoland during the NORDEX campaign in October 1996, J. Geophys. Res.-A, 105 (D18), 22 685–22 695, 2000.

Mentel, T. F., Sohn, M., and Wahner, A.: Nitrate effect in the heterogeneous hydrolysis of dinitrogen pentoxide on aqueous aerosols, Phys. Chem. Chem. Phys., 1 (24), 5451–5457, 1999.

Meixner, F. and Yang, W.: Biogenic Emissions of Nitric Oxide and Nitrous Oxide from Arid and Semi-Arid Land, Kluwer Academic Publishers, The Netherlands, 2004.

Platt, U. and Heintz, F.: Nitrate Radicals in Tropospheric Chemistry, Isr. J. Chem., 34 (3–4), 289–300, 1994.

Rinsland, C. P., Toon, G. C., Farmer, C. B., Norton, R. H., and Namkung, J. S.: Stratospheric N_2O_5 profiles at sunrise and sunset from further analysis of the ATMOS/Spacelab 3 solar spectra, J. Geophys. Res., 94 (D15), 18 341–18 349, 1989.

Robinson, G. N., Worsnop, D. R., Jayne, J. T., Kolb, C. E., and Davidovits, P.: Heterogeneous uptake of $ClONO_2$ and N_2O_5 by sulfuric acid solutions, J. Geophys. Res., 102 (D3), 3583–3601, 1997.

Sander, S. P., Friedl, R. R., Golden, D. M., Kurylo, M. J., Huie, R. E., Orkin, V. L., Moortgat, G. K., Ravishankara, A. R., Kolb, C. E., Molina, M. J., and Finlayson-Pitts, B. J.: Chemical Kinetics and Photochemical Data for Use in Atmospheric Studies, JPL Publication 02-25, Evaluation Number 14, 2003.

Sen, B., Toon, G. C., Osterman, G. B., Blavier, J. F., Margitan, J. J., Salawitch, R. J., and Yue, G. K.: Measurements of reactive nitrogen in the stratosphere, J. Geophys. Res.-A, 103 (D3), 3571–3585, 1998.

Simpson, W. R.: Continuous wave cavity ring-down spectroscopy applied to in situ detection of dinitrogen pentoxide (N_2O_5), Rev. Sci. Ins., 74 (7), 3442–3452, 2003.

Spivakovsky, C. M., Logan, J. A., Montzka, S. A., Balkanski, Y. J., Foreman-Fowler, M., Jones, D. B. A., Horowitz, L. W., Fusco, A. C., Brenninkmeijer, C. A. M., Prather, M. J., Wofsy, S. C., and McElroy, M. B.: Three-dimensional climatological distribution of tropospheric OH: Update and evaluation (Review), J. Geophys. Res.-A, 105 (D7), 8931–8980, 2000.

Stutz, J., Alicke, B., Ackermann, R., Geyer, A., White, A., and Williams, E.: Vertical Profiles of NO_3, N_2O_5, O_3, and NO_x in the nocturnal boundary layer: 1. Observations during the Texas Air Quality Study 2000, J. Geophys. Res., 109 (D12306), doi:10.1029/2003JD004209, 2004.

Toon, G. C., Farmer, C. B., and Norton, R. H.: Detection of stratospheric N_2O_5 by infrared remote sounding, Nature, 319, 570–571, 1986.

Warneke, C., de Gouw, J. A., Goldan, P. D., Kuster, W. C., Williams, E. J., Lerner, B. M., Jakoubek, R., Brown, S. S., Stark, H., Aldener, M., Ravishankara, A. R., Roberts, M., Marchewka, M., Bertman, S., Sueper, D. T., McKeen, S. A., Meagher, J. F., and Fehsenfeld, F. C.: Comparison of daytime and nighttime oxidation of biogenic and anthropogenic VOCs along the New England coast in summer during New England Air Quality Study 2002, J. Geophys. Res., 109 (D10), D10309, doi:10.1029/2003JD004424, 2004.

Wayne, R. P., Barnes, I., Biggs, P., Burrows, J. P., Canosa-Mas, C. E., Hjorth, J., Le Bras, G., Moortgat, G. K., Perner, D., Poulet, G., Restelli, G., and Sidebottom, H.: The nitrate radical: physics, chemistry, and the atmosphere, Atmos. Envir., Part A (General Topics), 25A (1), 1–203, 1991.

Wood, E. C., Wooldridge, P. J., Freese, J. H., Albrecht, T., and Cohen, R. C.: Prototype for in situ detection of atmospheric NO_3 and N_2O_5 via laser-induced fluorescence, Env. Sci. Tech., 37 (24), 5732–5738, 2003.

Zhou, D. K., Bingham, G. E., Rezai, B. K., Anderson, G. P., Smith, D. R., and Nadile, R. M.: Stratospheric CH_4, N_2O, H_2O, NO_2, N_2O_5, and $ClONO_2$ profiles retrieved from cryogenic infrared radiance instrumentation for shuttle (CIRRIS 1A)/STS 39 measurements, J. Geophys. Res.-A, 102 (D3), 3559–3573, 1997.